ОБЪЕДИНЕННЫЙ
ИНСТИТУТ
ЯДЕРНЫХ
ИССЛЕДОВАНИЙ
ДУБНА

E1 - 10037

B.A.Shahbazian, P.P.Temnikov, A.A.Timonina,
A.M.Rozhdestvensky

INVESTIGATION OF NATURE OF ENHANCEMENTS OBSERVED IN Λp EFFECTIVE MASS SPECTRA

1976

E1 - 10037

B.A.Shahbazian, P.P.Temnikov, A.A.Timonina,
A.M.Rozhdestvensky

INVESTIGATION OF NATURE OF ENHANCEMENTS OBSERVED IN Λp EFFECTIVE MASS SPECTRA

Invited Report at the XVIII International Conference on High Energy Physics (Tbilisi, July 15-21, 1976)

Шахбазян Б.А., Темников П.П., Тимонина А.А., Рождественский А.М.

E1 - 10037

Исследование природы особенностей, обнаруженных в спектрах эффективных масс Λp

В работе показано, что ранее обнаруженные особенности в спектрах масс Λp могут быть объяснены особенностями в сечениях упругого рассеяния Λp и конверсионных процессов $\Lambda p \to \Sigma^0 p$ и $\Sigma N \to \Lambda p$.

Работа выполнена в Лаборатории высоких энергий ОИЯИ.

Препринт Объединенного института ядерных исследований

Дубна 1976

Shahbazian B.A., Temnikov P.P., Timonina A.A., Rozhdestvensky A.M.

E1 - 10037

Investigation of the Nature of Enhancements Observed in Λp Effective Mass Spectra

A mechanism of formation of the enhancements discovered in the Λp effective mass spectra has been proposed. In the frame of a model, developed with this end in view, the peak near the origin of the spectrum is due to the negative Λp scattering length effect. The peaks at 2127 MeV/c^2 and 2257 MeV/c^2 most probably are due to Λp elastic resonances. The enhancement at 2184 MeV/c^2 is explained as a kinematical effect arising in two-step Σ-hyperon creation and $\Sigma\Lambda$-conversion processes. The elastic Λp scattering effective cross sections, computed using the best fit parameters, are in satisfactory agreement with the measured ones in the relative momentum interval P_Λ =(0.1-2.0) GeV/c.

Preprint of the Joint Institute for Nuclear Research

Dubna 1976

1. INTRODUCTION

Investigation of the Λp effective mass spectra (performed at the Laboratory of High Energies, JINR) in collisions of 4.0 *GeV/c* momentum negative pions and neutrons of 7.0 *GeV/c* average momentum with carbon nuclei ^{12}C, have led to the discovery of peaks near the sum of the Λ-hyperon and proton masses, 2127, 2257 *MeV/c*^{2}, and an enhancement at an average mass value of ~ 2184 *MeV/c*^{2} /1/.

Some of these enhancements were also observed in a series of experiments performed with deuterium-filled bubble chambers exposed to K^--meson beams of p_K= = (0. -1.65) *GeV/c* momenta /2/ and in proton-proton collisions at (2.40 - 2.85) *GeV*, i.e., at energies not very far from the threshold of the $(\Lambda p K^+)$ final state /3/.

The first three peaks reveal a remarkable constancy of their positions and width irrespective of the collision energy, the nature of the projectile and that of the target. The details and the discussion can be found in the review article /1/.

From the analysis of these experiments one can conclude that the enhancements are observed in those reactions in which the created Σ, Λ-hyperons have a good chance to interact with nucleons in the final states formed.

This conclusion suggests that the peaks observed in the Λp effective mass spectra should be due to enhancements in the hyperon-nucleon interaction effective cross sections /1/.

In order to check this hypothesis, a model was developed which, first of all, satisfactorily describes the experimental inclusive Λp effective mass spectrum from the interactions of 7.0 *GeV/c* average momentum neutrons with carbon nuclei with one Λ-hyperon, one and two protons and other particles in the final states.

Secondly, the best fit parameters obtained in the Λp effective mass spectrum fit enabled us to compute the Λp elastic scattering effective cross section as a function of the incident Λ-hyperon momentum from the interval $p_\Lambda = (0.1 - 2.0)$ *GeV/c* in the proton rest system in satisfactory agreement with the directly measured $\sigma_\Lambda^{el}(p_\Lambda)$ cross section.

These results permitted us to perform the simultaneous Λp effective mass spectrum and Λp elastic scattering effective cross section for the $p_\Lambda = (0.1 - 2.0)$ *GeV/c* interval least-square fit.

The average polarization of Λ-hyperons presumed to be daughters of Λp systems within the limits of errors is zero.

The experiment has been performed with the aid of the 55 *cm* JINR propane bubble chamber. The details concerning the experiment have been given in previous publications /1/. It is worth mentioning, that one could identify the protons only in the momentum range $0.150 < p_p < 1.0$ *GeV/c* and Λ-hyperons with momenta $p_\Lambda > 0.150$ *GeV/c*.

2. DESCRIPTION OF THE MODEL

The model proposed is based on impulse approximation, which is valid in our case firstly because the neutron energy considerably exceeds the nucleon binding energy in the carbon nucleus and secondly because we consider only the low mass part (2053.859 - 2553.859) *MeV/c*^{2} (or the relative momentum interval $p_\Lambda = 0. - 2.0$ *GeV/c*) of the whole Λp effective mass spectrum which extends in this experiment up to ~ 4800 *MeV/c*^{2}.

The neutron-carbon ^{12}C nucleus interaction in this approximation is considered as an interaction of the incident neutron with one of the nucleons forming a Fermi gas of nucleons with the momentum distribution coinciding with that measured in the experiment /5/.

Let us consider the most importan reactions of interaction of incident neutrons with moving nucleons leading to the final states Λp + (anything), Λpp + (anything).

2.1. Nuclear Cascade Processes

One can easily imagine nuclear cascade processes, initiated by an incident neutron, and terminating in these final states.

Let, for instance, in the first stage the incident neutron creates on a moving nucleon a Λ-hyperon. The hyperon leaves the nucleus not interacting with protons. In the second stage one of the accompanying particles (n , π , K) creates a proton in a collision with another moving nucleon. This secondary proton can leave the nucleus either with or without subsequent interaction with nucleons and can be identified in propane if its momentum satisfies the condition $0.15 < p_p < 1.0$ *GeV/c*. By analogy, one can imagine a nuclear cascade process in which, instead of Λ, a Σ-hyperon is created which can decay inside or even outside the nucleus into a pair of Λ-hyperon and γ-quantum.

Of course, the hyperon can be created in the second stage by one of the secondaries coming from the first stage which does not contain Λ-hyperon.

But the most important peculiarity of the above-considered nuclear cascade processes is a very low probability of the interaction of a Λ-hyperon either directly produced or resulting in the decay of a Σ°-hyperon with a proton emitted in another stage of the nuclear cascade process. This probability is much lower than that of interaction of the same Λ-hyperon with a proton of the nucleus.

The last circumstance stipulates much more feeble correlations between the Λ-hyperons and protons created

in nuclear cascade processes in comparison with the correlations arising in the below considered $\Lambda p \to \Lambda p$, $\Sigma N \to \Lambda p$ two-body reactions.

As far as at the present time it is impossible to compute exactly hadronic effective cross sections, we always use all the available experimental information on production and interactions of strange particles in elementary acts.

This is admissible inasmuch as the impulse approximation is. Accordingly we treat the totality of Λ-hyperons produced in propane (i) on free and quasi-free protons (the total final state electric charge $Q = 1$), (ii) on neutrons ($Q = 0$) and (iii) in nuclei ($Q > 1$), the events of all three classes not containing protons of momenta $0.15 < p_p < 1.0$ *GeV/c* identical with the totality of Λ-hyperons created in carbon nuclei but which have not suffered subsequent intranuclear interactions. In a part of events created on quasi-free protons and neutrons, as well as in nuclei, the Λ-hyperons could be produced in the second stage, i.e., by particles, produced in the first stage. The number of Λ-hyperons of all three classes in our experiment is equal to 1311. This sample contains also Λ-hyperons from the 69 $\Sigma^\circ \to \Lambda\gamma$ decays. As nuclear cascade protons, the proton from the events contributing to the experimental Λp effective mass spectrum have been taken.

Having the models of samples of the nuclear cascade Λ-hyperons and protons, one can easily obtain the corresponding Λp effective mass spectrum of lambdas and protons, which have never interacted with each other, computing and histogramming effective masses of each Λp pair $\Phi(M_{\Lambda p})$. The probability of this nuclear cascade background in the $(M^i_{\Lambda p}, M^{i+1}_{\Lambda p})$ mass interval is equal to

$$\phi^{i,i+1}(M_{\Lambda p}) = \frac{\Phi_i(M_{\Lambda p})}{\sum_{i=1}^{n_{max}} \Phi_i(M_{\Lambda p})}, \qquad (1)$$

2.2. Hyperon-Nucleon Interactions

A part of the Λ- and Σ-hyperons, created in a carbon ^{12}C nucleus can interact with its s- and p-shell nucleons, providing in this way the final states with lambdas and protons.

The highest limit of the Λp experimental effective mass spectrum $M^{max}_{\Lambda p} = 2553.859$ *MeV/c*^{2} has been chosen in order to ensure relatively low statistical fluctuations in the distant part of the spectrum.

The corresponding Λ-hyperon momentum in the proton rest system is equal to $p_\Lambda = 2.0$ *GeV/c*.

Therefore one should model the most important intranuclear hyperon-nucleon interaction processes in the incident Λ-hyperon momentum interval $p_\Lambda = (0. - 2.0)$ *GeV/c*, the detection of the corresponding events in the propane bubble chamber taking into account its geometrical form and dimensions, the beam geometry, as well as accounting for the kinematical restrictions.

The elastic Λp scattering effective cross section dominates in the $p_\Lambda = (0. - 2.0)$ *GeV/c* interval. The next are the cross sections of $\Lambda p \to \Sigma^\circ p$; $\overset{+}{\Sigma}{}^\circ N \to \Lambda p$ two-body processes /4/.

The thresholds of inelastic processes $\Lambda p \to \Lambda p \pi^\circ$, $\Lambda p \to \Lambda p \pi^+ \pi^-$, etc., are situated at Λp effective mass values higher than the average mass of the last peak at ~2257 *MeV/c*^{2}, and the corresponding effective cross sections are up to $M^{max}_{\Lambda p}$ so small that the accounting for them would result in corrections which are within the experimental errors.

Therefore we have limited ourselves considering only the following two-body processes: $\Lambda p \to \Lambda p$; $\Lambda p \to \Sigma^\circ p$, $\overset{+}{\Sigma}{}^\circ N \to \Lambda p$.

These processes have been modelled, colliding the mentioned 1311 Λ- and 69 Σ°-hyperons with moving nucleons.

(i) Λ-hyperon-proton elastic scattering is assumed to proceed via resonant and nonresonant or potential scattering channels.

The effective cross section is assumed to be equal to

$$\sigma^{e\ell}_{\Lambda p}(M'_{\Lambda p}) = \sigma_1(M'_{\Lambda p}) + \sigma_2(M'_{\Lambda p}) + \sigma_3(M'_{\Lambda p}) + \sigma_4(M'_{\Lambda p}) \qquad (2)$$

neglecting the interference terms and using the isolated resonance approximation.

Here

$$\sigma_1(M'_{\Lambda p}) = \frac{4\pi}{(-\frac{1}{a} + \frac{r}{2}k^2(M'_{\Lambda p}))^2 + k^2(M'_{\Lambda p})} \qquad (3)$$

accounts for the low energy Λp scattering assuming in singlet and triplet states equal scattering parameters, i.e., $a_s = a_t = a$, $r_s = r_t = r$. In order to describe the peaks at 2127 and 2257 MeV/c^2, two Breit-Wigner terms for elastic scattering Λp resonances have been introduced /6/

$$\sigma_{2,3}(M'_{\Lambda p}) = \frac{4\pi(2J_{\Lambda p}+1)M^2_{R_{2,3}}\Gamma^2\chi^2}{p^{*2}(2J_\Lambda+1)(2J_p+1)[(M^2_{R_{2,3}} - M'^2_{\Lambda p})^2 + M^2_{R_{2,3}}\Gamma^2]}, \qquad (4)$$

where $\chi = \hbar c$,

$$\Gamma = (\frac{p^*}{p^*_{R_{2,3}}})^{2\ell+1}\Gamma_{R_{2,3}}.$$

Taking $J = \ell = 0$, one has

$$\sigma_{2,3}(M'_{\Lambda p}) = \frac{\pi\chi^2 M^2_{R_{2,3}}\Gamma^2_{R_{2,3}}}{p^{*2}_{R_{2,3}}(M'^2_{\Lambda p} - M^2_{R_{2,3}})^2 + M^2_{R_{2,3}}\Gamma^2_{R_{2,3}}p^{*2}}, \qquad (5)$$

where

$$p^{*2} = \frac{1}{4M'^2_{\Lambda p}}\{(M'^2_{\Lambda p} - M^2_\Lambda - M^2_p)^2 - 4M^2_\Lambda M^2_p\}, \qquad (6)$$

$$p^{*2}_{R_{2,3}} = \frac{1}{4M^2_{R_{2,3}}}\{(M^2_{R_{2,3}} - M^2_\Lambda - M^2_p)^2 - 4M^2_\Lambda M^2_p\}. \qquad (7)$$

Let us now turn to the potential Λp scattering. As the corresponding matrix element varies with the relative momentum or the effective mass $M'_{\Lambda p}$ much slower than the resonance matrix elements do, it seems reasonable to assume the potential scattering effective cross section to be proportional to the Λp phase space volume.

$$\sigma_4(M'_{\Lambda p}) = \pi R^2 R_2(M'_{\Lambda p}). \qquad (8)$$

$$R_2(M'_{\Lambda p}) = \frac{\pi p^*}{M'_{\Lambda p}}, \qquad (9)$$

Here p^* is given by the formula (6), and R is an average range of the Λp interaction forces.

The probability of detection of intranuclear scattering events occurred in the bubble chamber volume whose effective masses contribute to the Λp spectrum bin $(M^{\Lambda p}_i, M^{\Lambda p}_{i+1})$, at finite mass resolution, is expressed as

$$W^{i,i+1}_{e\ell}(M_{\Lambda p}) = N_{e\ell}\{\int_{M^{\Lambda p}_i}^{M^{\Lambda p}_{i+1}} dM_{\Lambda p}(\int_{M_{\Lambda p}-3\Delta_1}^{M_{\Lambda p}+3\Delta_1} w_1(M'_{\Lambda p})J(M'_{\Lambda p})e^{-\frac{(M_{\Lambda p}-M'_{\Lambda p})^2}{2\Delta_1^2}} dM'_{\Lambda p} +$$

$$+\int_{M_{\Lambda p}-3\Delta_2}^{M_{\Lambda p}+3\Delta_2} w_2(M'_{\Lambda p})J(M'_{\Lambda p})e^{-\frac{(M_{\Lambda p}-M'_{\Lambda p})^2}{2\Delta_2^2}}dM'_{\Lambda p} +$$

$$+\int_{M_{\Lambda p}-3\Delta_3}^{M_{\Lambda p}+3\Delta_3} w_3(M'_{\Lambda p})J(M'_{\Lambda p})e^{-\frac{(M_{\Lambda p}-M'_{\Lambda p})^2}{2\Delta_3^2}}dM'_{\Lambda p}) + \qquad (10)$$

$$+\int_{M_i^{\Lambda p}}^{M_{i+1}^{\Lambda p}} w_4(M'_{\Lambda p})J(M'_{\Lambda p})dM'_{\Lambda p}\}.$$

Here $w_m(M'_{\Lambda p})$, $m = 1,2,3,4$ are the normalized to one effective cross section contributions

$$w_{1,2,3}(M'_{\Lambda p}) = \sigma_{1,2,3}(M'_{\Lambda p})\left(\int_{M_\Lambda+M_p}^{M_{\Lambda p}^{max}} \sigma_{\Lambda p}^{e\ell}(M'_{\Lambda p})dM'_{\Lambda p}\right)^{-1};$$

$$w_4(M'_{\Lambda p}) = \sigma_4(M'_{\Lambda p})\left(\int_{M_\Lambda+M_p}^{M_{\Lambda p}^{\ell im}} \sigma_{\Lambda p}^{e\ell}(M'_{\Lambda p})dM'_{\Lambda p}\right)^{-1}, \qquad (11)$$

$N_{e\ell}$ is the normalization factor equal to the reciprocal of the quantity $W_{e\ell}^{st}$ where s corresponds to the $M_\Lambda + M_p =$ $= 2053.859$ *MeV/c*^{2} and f to the accepted limiting value $M_{\Lambda p}^{\ell im} = 3553.859$ *MeV/c*^{2} which results in $N_{e\ell}$ about 1% larger than for the kinematical limit; $\Delta_1 =$ $=3.00$ *MeV/c*^{2}; $\Delta_2 = 4.25$ *MeV/c*^{2}; $\Delta_3 = 6.40$ *MeV/c*^{2} are the standard deviations of the resolution function in the domains of the peaks; $J(M'_{\Lambda p})$ is the flux-factor with the account for the probability of detection of the Λ-intranuclear proton elastic scattering events as a function of the effective mass $M'_{\Lambda p}$ of colliding particles.

The last integrand in formula (10) is a slowly varying function and thereby do not need for Gaussian convolution.

(ii) The probability of the occurrence and detection in the chamber of a sequence, the intanuclear $\Lambda p \to \Sigma^\circ p$ conversion and $\Sigma^\circ \to \Lambda\gamma$ decay processes as a function of the final state $M'_{\Lambda p}$ effective mass values contributing to the $(M_i^{\Lambda p}, M_{i+1}^{\Lambda p})$ histigramm bin with the finite effective mass resolution taken into account, is expressed as

$$W_{\Lambda\Sigma\Lambda}^{i,i+1}(M_{\Lambda p}) = N_{\Lambda\Sigma\Lambda}\int_{M_i^{\Lambda p}}^{M_{i+1}^{\Lambda p}} dM_{\Lambda p}\int_{M_{\Lambda p}-3\Delta_3}^{M_{\Lambda p}+3\Delta_3} J_{\Lambda\Sigma\Lambda}(M'_{\Lambda p})e^{-\frac{(M_{\Lambda p}-M'_{\Lambda p})^2}{2\Delta_2^2}}dM'_{\Lambda p}. \qquad (12)$$

Here $N_{\Lambda\Sigma\Lambda}$ is the normalizing factor; $J_{\Lambda\Sigma\Lambda}(M'_{\Lambda p})$ is the probability of the occurrence and detection in the chamber volume of a sequence of processes $\Lambda p \to \Sigma^\circ p$, $\Sigma^\circ \to \Lambda\gamma$ as a function of the effective mass $M'_{\Lambda p}$ of the final state proton and Λ-hyperon.

(iii) By analogy, for the last intranuclear processes $\Sigma^\circ N \to \Lambda p$ one has

$$W_{\Sigma\Lambda}^{i,i+1}(M_{\Lambda p}) = N_{\Sigma\Lambda}\int_{M_i^{\Lambda p}}^{M_{i+1}^{\Lambda p}} dM_{\Lambda p}\int_{M_{\Lambda p}-3\Lambda_3}^{M_{\Lambda p}+3\Lambda_3} J_{\Sigma\Lambda}(M'_{\Lambda p})e^{-\frac{(M_{\Lambda p}-M'_{\Lambda p})^2}{2\Lambda_3^2}}dM'_{\Lambda p}. \qquad (13)$$

3. *RESULTS*

If the total number of Λp combinations in the experimental effective mass spectrum is N_0, the predicted number of events contributing to $(M_i^{\Lambda p}, M_{i+1}^{\Lambda p})$ bin is read as

$$N_{i,i+1}^{Th}(M_{\Lambda p}) = N_0\{AW_{e\ell}^{i,i+1}(M_{\Lambda p}) + BW_{\Lambda\Sigma\Lambda}^{i,i+1}(M_{\Lambda p}) +$$

$$+ CW_{\Sigma\Lambda}^{i,i+1}(M_{\Lambda p}) + D\phi^{i,i+1}(M_{\Lambda p})\}. \qquad (14)$$

The best fit parameters a, r, M_{R_2}, Γ_{R_2}, M_{R_3}, Γ_{R_3}, A, B, C, D, R for the minimum of the functional

$$\chi^2_n = \sum_{i=1}^{k} \frac{(N^{exp}_{i,i+1} - N^{Th}_{i,i+1})^2}{N^{exp}_{i,i+1}} + 2a(1-Q) \qquad (15)$$

with a constraint imposed on the contributions

$$Q \equiv A + B + C + D = 1 \qquad (16)$$

have been found.

Here $N^{exp}_{i,i+1}$ is the height of the column of the experimental histogram in $(M^{\Lambda p}_i, M^{\Lambda p}_{i+1})$ bin, a is the Lagrange multiplier.

In order to ensure the minimal number of events in a bin to be no less than twenty, we had to combine several 5 MeV/c^2 bins in the distant part of the effective mass spectrum.

Thus, instead of 50 bins, 10 MeV/c^2 each, we have $k = 45$ unequal bins. So the number of degrees of freedom is $n = 34$.

The simplest model (only the intranuclear cascade processes are important) does not fit the experiment giving $\chi^2_{44} = 121.6$.

The resulting histogram of the complete model fit is shown in the upper part of *fig. 1* by open circles. The best fit parameters in the second column of table 1 are presented ($M_{\Lambda p}$ - fit). Of course, the obtained high confidence level itself cannot serve as a proof of correctness of the model. For this purpose one needs an independent check and proof. With this end in view, using the best fit parameters and (2)-(9) formulae, the Λp elastic scattering effective cross sections have been computed and averaged over the momentum intervals accepted in the experiments [4].

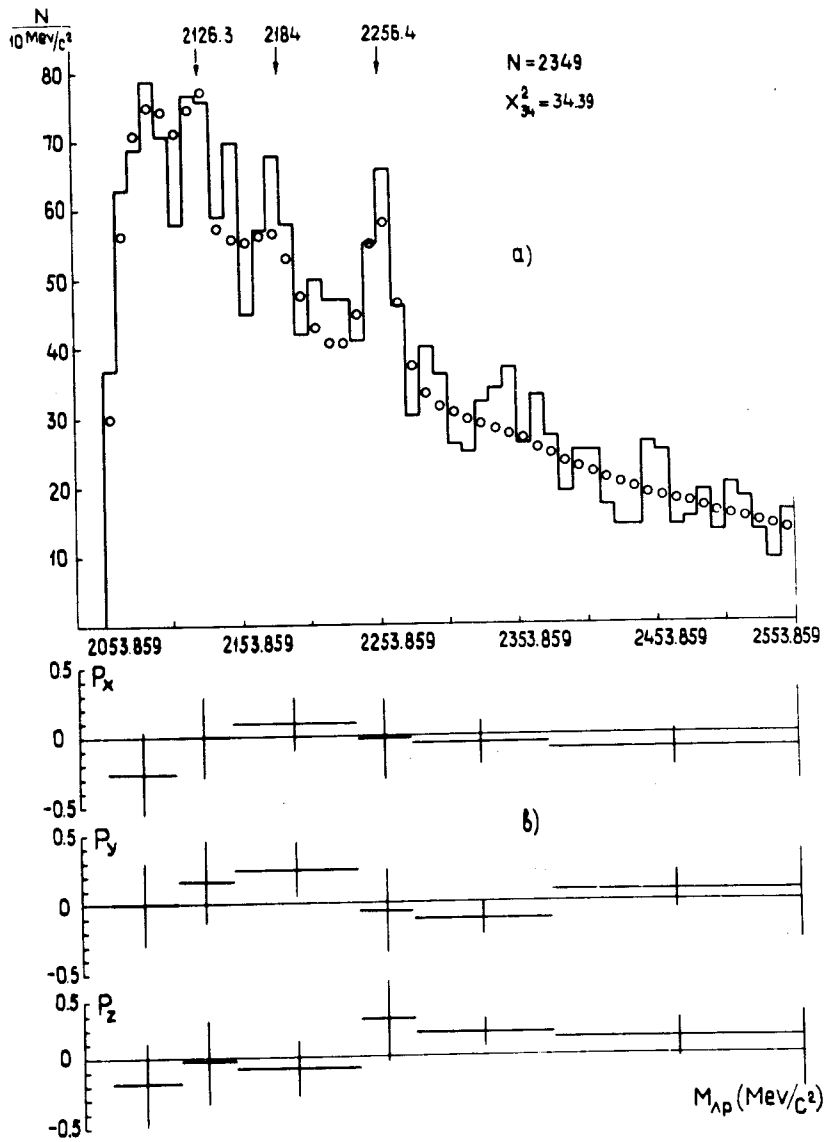

Fig. 1.a) The Λp effective mass spectrum from 1115 Λp and 617 Λpp inclusive final states. The open circles represent the histogram fitted to the experimental one.

b) The components of average polarization of Λ - hyperons presumed to be daughters of Λp-systems.

Table I. The results of fitting

	$M_{\Lambda p}$-fit	$(M_{\Lambda p}+\sigma^{el}_{\Lambda p})$-fit	$(M_{\Lambda p}+\sigma^{el}_{\Lambda p})$-fit for isotropic c.m.s. distributions over $\cos\theta_{\Lambda\Lambda}$, $\cos\theta_{\Lambda\Sigma}$, $\cos\theta_{\Sigma\Lambda}$
χ^2_n	χ^2_{34}=34.39	χ^2_{55}= 59.69	χ^2_{55}= 59.57
C.L. (%)	44.92	31.56	31.92
a (fm)	-2.30 ± 0.35	-2.39 ± 0.04	-2.38 ± 0.05
r (fm)	4.73 ± 0.50	4.87 ± 0.05	4.82 ± 0.06
M_2(MeV/c^2)	2126.30 ± 1.66	2127.00 ± 3.38	2127.60± 2.29
Γ_2(MeV/c^2)	3.78 ± 0.92	3.76 ± 0.96	3.94 ± 1.00
M_3(MeV/c^2)	2256.40 ± 3.12	2256.90 ± 1.33	2256.80± 2.86
Γ_3(MeV/c^2)	15.97 ± 4.40	15.55 ± 4.20	17.05 ± 4.55
A($\Lambda p\to\Lambda p$)	0.332 ± 0.008	0.336 ± 0.005	0.345 ± 0.018
B($\Lambda p\to\Sigma^0 p$)	0.117 ± 0.005	0.109 ± 0.003	0.099 ± 0.021
C($\Sigma\Lambda$)	0.081 ± 0.004	0.083 ± 0.004	0.083 ± 0.023
D(i.c.b.)*)	0.469 ± 0.004	0.471 ± 0.005	0.471 ± 0.026
R(fm)	0.659 ± 0.020	0.664 ± 0.015	0.666 ± 0.025

*) i.c.b. - intranuclear cascade background

These results are shown in *fig. 2* by open circles and agree with the directly measured Λp elastic scattering cross section at 12% confidence level.

The negative low energy Λp scattering length manifests itself as the peak near the Λp threshold of the effective mass spectrum (*fig. 1*) and as the decreasing part of the elastic scattering cross section in the low energy region (*fig. 2*).

The resonance Λp scattering manifests itself in the effective mass spectrum as two peaks at 2127 and 2257 *MeV/c*^{2} mass values and as irregularities of the averaged Λp elastic scattering effective cross section in the Λ-hyperon relative momentum intervals (0.6 - - 0.7) *GeV/c* and (1.0 - 1.2) *GeV/c* (*fig. 2*).

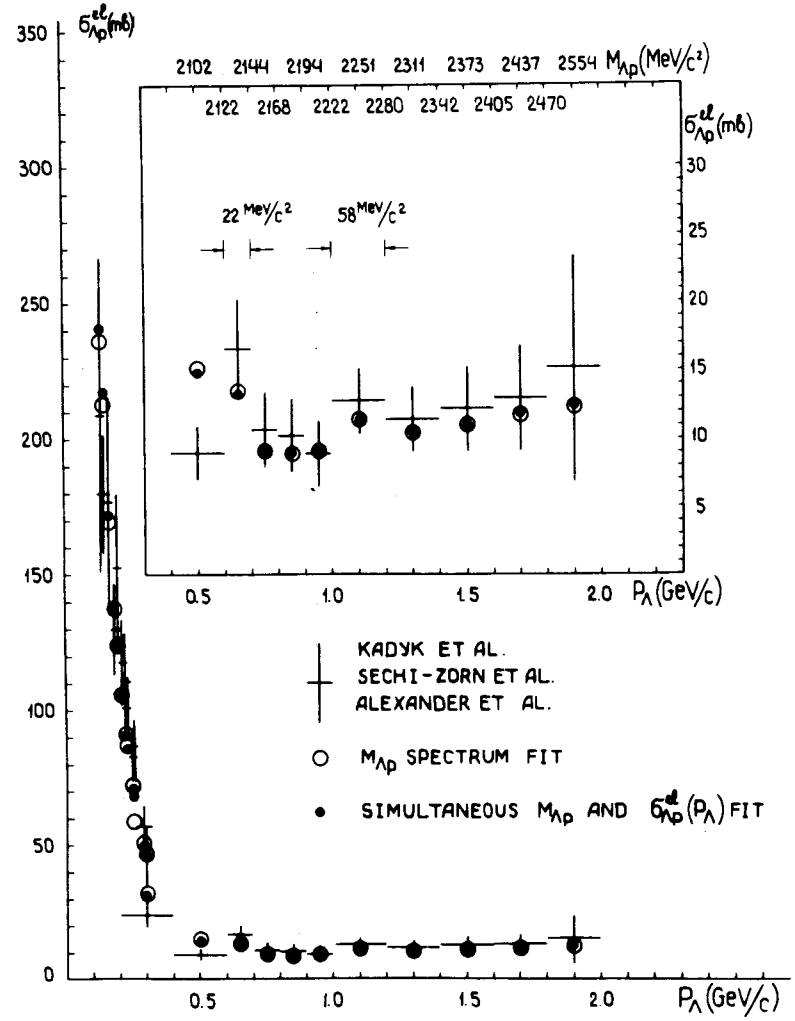

Fig. 2. The average Λp elastic scattering effective cross sections in the Λ-hyperon relative momentum interval p_Λ = (0.1 - 2.0) GeV/c. The crosses are due to the direct measurements of the average cross sections /4/. The open circles represent the predicted average cross sections due to the fit to the effective mass spectrum only. The blackened circles refer to the results of the same kind due to the simultaneous fit to the Λp effective mass spectrum and effective cross sections.

The reasonable value of the obtained potential scattering parameter R permits one to describe correctly the high energy part of the Λp-scattering cross section.

Thus, one can state that the model describes correctly in broad outline the results if Λp enhancement production and formation experiments, and particularly the elastic scattering effective cross section in the Λ-hyperon relative momentum interval $p_\Lambda = (0.1\text{–}2.0)$ *GeV/c*.

These results encouraged us to perform a simultaneous fit of the Λp effective mass spectrum and elastic scattering effective cross section.

In this case the minimum of the functional

$$\chi^2_n = \sum_{i=1}^{k} \frac{(N^{exp}_{i,i+1} - N^{Th}_{i,i+1})^2}{N^{exp}_{i,i+1}} + \sum_{j=1}^{\ell} \frac{(\sigma^{exp}_{\Lambda p}(p_\Lambda) - \sigma^{Th}_{\Lambda p}(p_\Lambda))^2_j}{(\Delta\sigma^{exp}_{\Lambda p}(p_\Lambda))^2_j} + 2\alpha(1 - G) \qquad (17)$$

has been searched for.

The total number of points becomes now equal to 68 ($k = 45, \ell = 23$) and the number of degrees of freedom at 11 parameters is equal to $n = 55$.

The results of this simultaneous fit are shown in *figs. 2* and *3* by black points and in the third column of table 1 ($(\sigma^{el}_{\Lambda p} + M_{\Lambda p})$-fit).

The components of the black-point histogram due to all the above-considered processes are presented by the corresponding histograms in *fig. 3*. It is clearly seen that the three resonance peaks are backed by the background composed of four components. These are the contributions due to the Λp potential scattering, $\Lambda\Sigma$ - and $\Sigma\Lambda$ conversion and intranuclear cascade processes.

The 2184 *MeV/c*^{2} enhancement is due to the $\Sigma\Lambda$-conversion process. The computed and measured Λp elastic scattering effective cross sections agree at 27% confidence level.

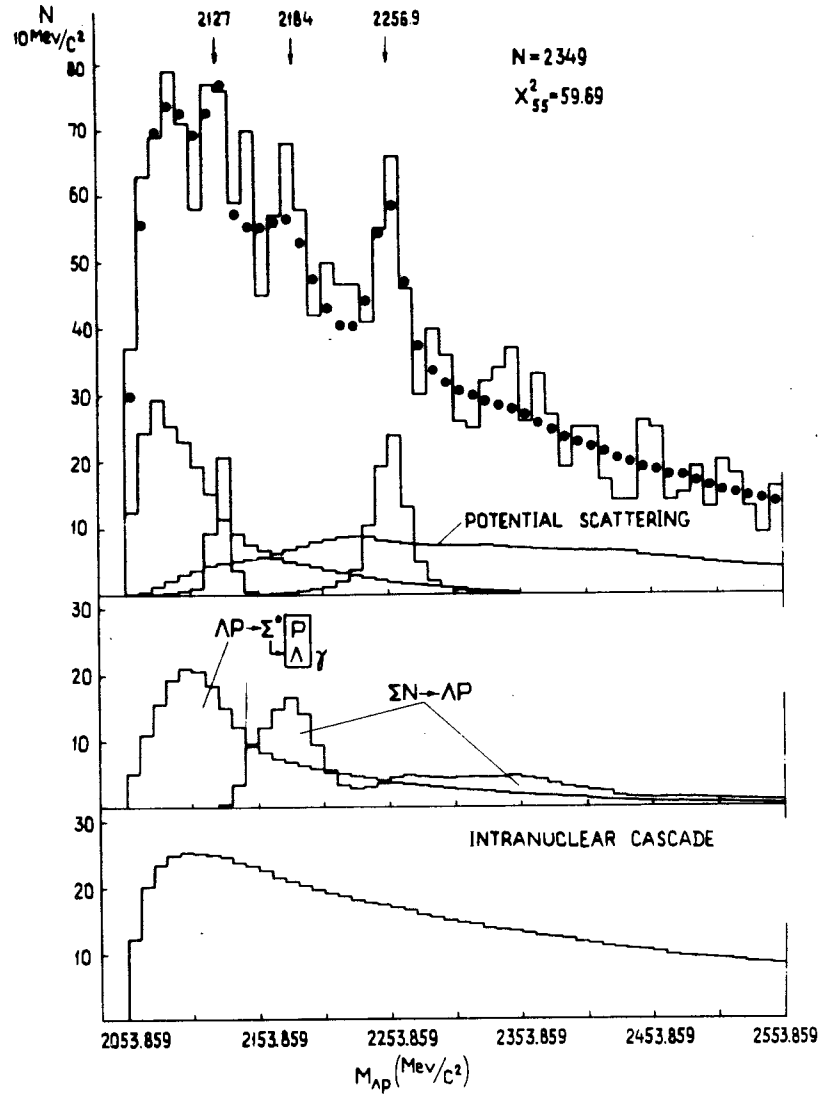

Fig. 3. Results of the simultaneous fit to the Λp effective mass spectrum and elastic scattering effective cross sections. The summary histogram (blackened circles) and the contributing histograms corresponding to various processes are shown.

As mentioned above, the model uses the experimental c.m.s. angular distributions of two-body $\Lambda p \to \Lambda p$, $\Lambda p \to \Sigma^0 p$ and $\Sigma N \to \Lambda p$ processes measured with rather large errors.

Then a quite natural question arises how the final results would change if these angular distributions were substantially changed.

Remembering that the only quantities depending on them are the $J(M'_{\Lambda p})$, $J_{\Lambda\Sigma\Lambda}(M'_{\Lambda p})$ and $J_{\Sigma\Lambda}(M'_{\Lambda p})$ functions, we have changed the measured c.m.s. angular distributions for the isotropic ones. The results of the fit performed now for the isotropic c.m.s. angular distributions coincide with the old ones within the limits of errors.

This result should be expected for the following reasons.

Firts, due to the low efficiency for the detection of fast Λ-hyperons and protons, the bubble chamber selects events of like configurations in laboratory system irrespective of the initial c.m.s. angular distribution.

Thus, the effective c.m.s. angular distributions selected from both initial distributions, the measured forward-peaked and the isotropic ones, should not differ substantially from each other.

Then one should expect only negligible difference in the functions $J(M'_{\Lambda p})$, $J_{\Lambda\Sigma\Lambda}(M'_{\Lambda p})$ and $J_{\Sigma\Lambda}(M'_{\Lambda p})$ computed for these two different c.m.s. angular distributions.

Indeed, these expectations are very well supported by the comparison.

Second, the Gaussian convolutions and integrations over the histogram bins performed in formulae (10), (11) and (13), smooth over the differences still more.

More generally, the probabilities (10), (12) and (13) strongly depend on rapidly varying effective cross sections (11) and on Gaussian functions and only very weakly-on c.m.s. angular distributions.

Thus, the differences of the results of two fits wear off as one can see when comparing the third and fourth columns of table 1.

Table 2. Investigation of the necessity of accounting for various processes

Without accounting for the		Confidence level (%)
Low energy Λp scattering	$\chi^2_{57} = 584.2$	-
resonances at 2127 MeV/c^2 and 2257 MeV/c^2	$\chi^2_{59} = 87.5$	0.9
resonance at 2257 MeV/c^2	$\chi^2_{57} = 82.0$	1.6
resonance at 2127 MeV/c^2	$\chi^2_{57} = 68.9$	12.0
potential scattering	$\chi^2_{56} = 144.6$	-
$\Lambda\Sigma$-conversion	$\chi^2_{56} = 79.8$	1.9
$\Sigma\Lambda$-conversion	$\chi^2_{56} = 68.8$	10.0
intranuclear cascade	$\chi^2_{56} = 86.3$	0.5

In order to investigate the necessity of accounting for the processes considered, a simultaneous $(\sigma^{\ell}_{\Lambda p} + M_{\Lambda p}$ - fit with "turned off" various processes has been performed. The results are presented in table 2.

The first peak, which is due to the low energy Λp scattering with the negative scattering length, is quite necessary.

This result is stipulated by six histogram bins of the Λp effective mass spectrum and thirteen measured values of the Λp elastic scattering effective cross section.

The necessity of negative sign of the Λp scattering length is proved by starting the fitting procedure at a positive scattering length value. The minimum is reached only at negative sign values as is seen in *fig. 4*. When the error of the positive starting scattering length is set very small, the χ^2_n decreases tending to saturation at about 300 and $r \approx 10$ *fm* (the upper part of *fig. 4*). But for larger errors, the scattering length suddently changes the sign to the negative one and reaches the minimum of $\chi^2_{55} \approx 60$. at reasonable values of a and r (the lower part of *fig. 4*).

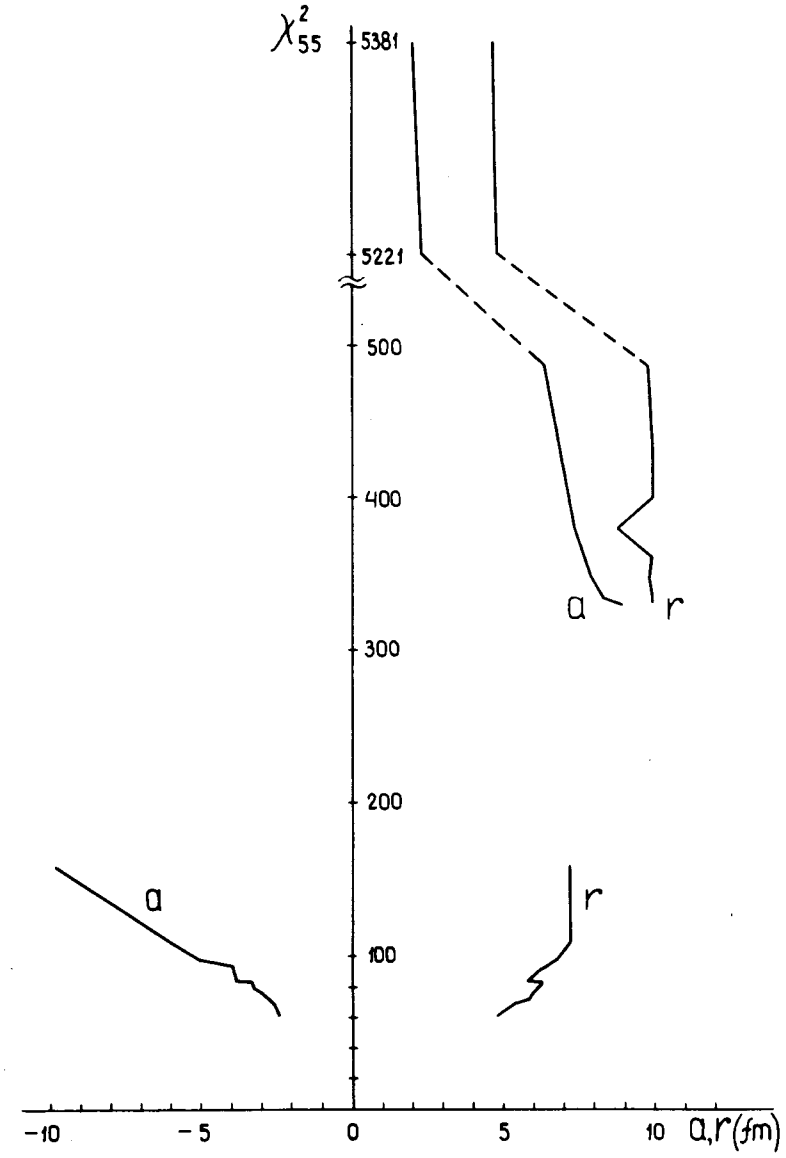

Fig. 4. The dependence of χ^2_{55} *on the sign of the low energy* Λp *scattering length.*

It is obvious that the confidence levels for the third and especially for the second narrow peaks would be much higher than it follows from table 2 if the measurements of the effective cross sections and their averaging over much narrower momentum intervals were performed. Also, a higher number of effective mass bins would be desirable in the vicinity of these peaks, especially of the second peak.

This can be clearly seen in *fig. 5* where the predicted by the model and the measured Λp elastic scattering average effective cross sections are presented.

The peak at 2257 *MeV/c*^{2} most probably is due to the Λp resonance of this mass. At present we do not see any alternative for this peak. The model predicts this resonance to be formed with effective cross section $\sigma^{el}_{\Lambda p}(1120) = 5.61$ *mb.*

The situation with the peak at 2127 *MeV/c*^{2} is more complicated mainly because it is situated very near the ΣN threshold. This means that besides the Λp resonance in the pure elastic scattering channel one should take into account the influence of coupling effects of the $\Lambda p \to \Lambda p$ and $\Sigma N \to \Lambda p$ channels.

The second cause has not been considered in this work because the corresponding analysis would need for several tens of bins in an interval of about 40 *MeV/c*^{2} in the region of this peak. Experiments of other types seem to be more fruitful, especially those studying with high precision the behaviour of the Λp cross section in the vicinity of ΣN threshold.

Note that an attempt /7/ has been made to explain this peak as a kinematical effect due to the two-step process for the reaction $K^- d \to \Lambda p \pi^-$, namely

$K^- d \to (\Sigma N)\pi^-$ followed by $\Sigma N \to \Lambda p$.

This two-step model has been calculated using the deuteron wave function and the experimental differential and total cross sections of the intermediate reaction $K^- N \to \Sigma^\circ \pi^-$. For the second step a constant $\Sigma\Lambda$-conversion matrix element has been assumed, i.e., the cross section has been assumed to be proportional to the phase space divided by incoming flux.

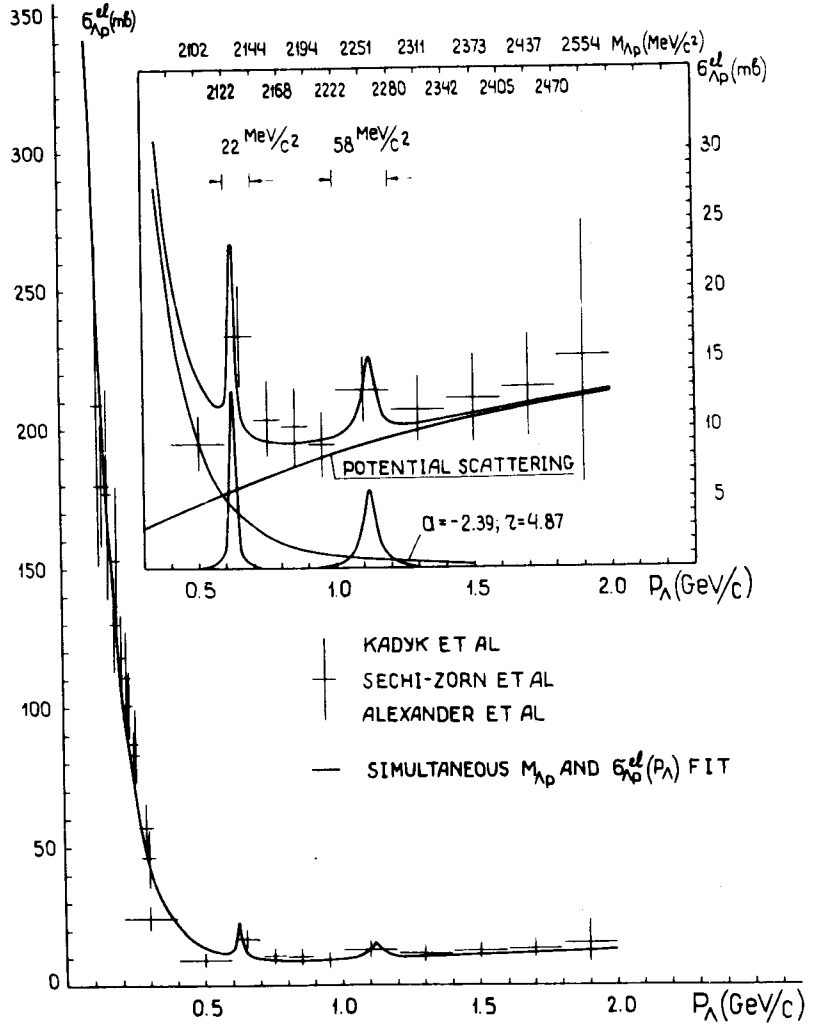

Fig. 5. The predicted by our model unaveraged Λp *elastic scattering effective cross section as a function of the* Λ*-hyperon relative momentum in the interval* p_Λ = *(0.1 - 2.0) GeV/c. The best fit parameters used are the same as for the computed average cross sections (blackened circles in fig. 2). But the cross sections now have not been averaged over the momentum intervals accepted in the direct experiments, the results of which, average cross sections, are presented by crosses. The horizontal bars of crosses represent the momentum intervals over which the averaging is made.*

The model predicts, indeed a peak slowly moving to higher masses with an increase of the incident K-meson momentum.

Its positions are at mass values somewhat higher that the experimental one and also the width do not agree with the observed widths.

We have repeated these calculations for the K^-d and $n\,^{12}C$ interactions. The K^-d calculations differ from those referred to above in the use of corresponding experimental differential and total cross sections in the second stage also. The calculations have been performed for K-meson momenta $p_{K^-} = 0$ and $p_{K^-} = (1.45 - 1.65)$ *GeV/c*.

The $^{12}C \to (\Sigma N) +$ (anything) and $\Sigma N \to \Lambda p$ two-step reaction probability coincides with the above calculated conversion probability $W_{\Sigma\Lambda}(M'_{\Lambda p})$ (see formula (13)).

All three histograms in 2 *MeV/c*^{2} bins are presented in *fig. 6*.

One can see that the peak is both moving towards higher masses and broadening faster than in /7/.

As said above, we identify the 2184 *MeV/c*^{2} enhancement with the kinematical peak due to the $\Sigma\Lambda$-conversion (*figs. 3* and *6*).

Hence the possibility of the kinematical origin of the 2127 *MeV/c*^{2} peak is completely ruled out. Moreover, the "shoulder" at 2138 *MeV/c*^{2} observed in the Λp effective mass spectrum in the $K^-d \to \Lambda p\pi^-$ reaction initiated by stopping K^--mesons /2/ may be well due to the same kinematic effect as is seen in *figs. 3* and *6*.

Thus, the 2127 *MeV/c*^{2} peak should be considered as a Λp elastic resonance originating from the Λp resonance scattering and the coupling effects of the $\Lambda p \to \Lambda p$ and $\Sigma N \to \Lambda p$ channels. The contribution of the second effect could not be determined in this experiment.

The results obtained and the precision of this experiment justify main approximations made. The resonance formation effective cross section predicted by our model is $\sigma^{el}_{\Lambda p}(620) = 12.86$ *mb*.

We have neglected all interference terms in formula (2).

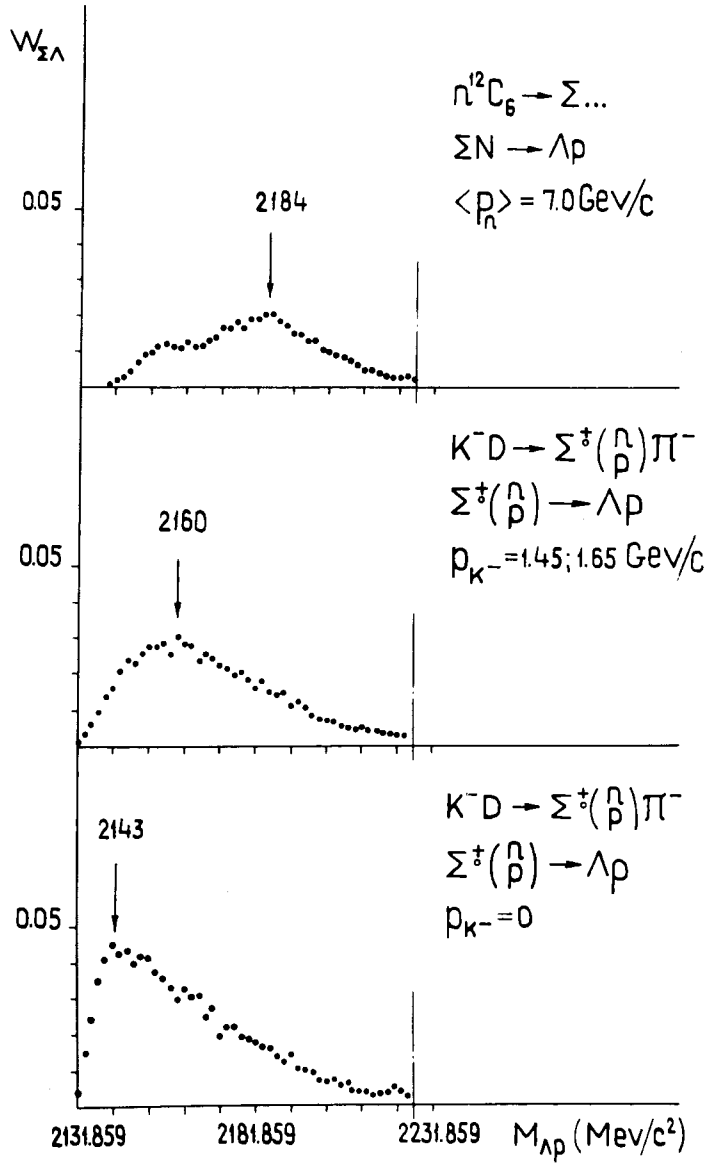

Fig. 6. The Λp ***effective mass spectrum provocated by the two-step*** Σ ***-hyperon creation and*** $\Sigma\Lambda$ ***conversion processes.***

The neglect of the terms arising from the interference of the two resonance amplitudes with each other and each of them with the potential and low energy scattering amplitudes is justified for narrow resonances as in our case.

In their turn, the amplitudes of the potential and low energy scattering, which vary in opposite ways, give also a negligible interference term. By all the enumerated reasons the use of isolated resonance approximation and formula (2) is justified [9].

Finally, as the conversion reaction $\Lambda p \to \Sigma^0 p$ cross sections are much lower in the resonance regions than the elastic scattering effective cross section, we assume $\Gamma_{tot} \approx \Gamma_{el} = \Gamma_R$ and use formulae (4) and (5) as for the purely elastic scattering resonance cross section.

The determination of the spins and parities of resonances possibly observed in this experiment, reduces to the spin-parity analysis for bosons decaying into spin $-1/2$ pairs [8].

The condition that the spin and parity of the Λp -system be uniquely determined are that some spin-correlation terms in the full triple angular distribution are measured.

If the spin projections of Λ -hyperons and protons are not measured, the spin and parity of the Λp -system, cannot, in general, be fixed.

These conditions could not be fulfilled in this experiment.

Only the components of the average polarization of Λ -hyperons, presumed to be daughters of a Λp-system along the beam direction $- P_z$, normal to the Λp -production plane $- P_y$ and normal to both these directions $- P_x$, have been measured.

In the lower part of *fig. 1* one can see that all three components within the limits of errors are zero.

4. CONCLUSIONS

The inclusive Λp effective mass spectrum from the interactions of 7 *GeV/c* average momentum neutrons with

carbon nuclei has been investigated. Four enhancements have been discovered in it.

The comparison of physical and experimental conditions at which these peaks have been observed in this and other experiments [1-3], suggests that they should be the manifestations of peculiarities of the Λp elastic scattering and $\Lambda\Sigma$- and $\Sigma\Lambda$-conversion effective cross sections.

To analyze this hypothesis, a model of creation and interactions of Λ- and Σ-hyperons in carbon nuclei, bombarded with 7 *GeV/c* average momentum neutrons, has been developed.

The model is based on impulse approximation.

1. The analysis, performed in the frame of this model, permitted us to sucessfully describe not only the Λp effective mass spectrum with its enhancements, i.e., the results of the Λp enhancement production experiment but also the behaviour of the Λp elastic scattering effective cross section in the Λ-hyperon relative momentum interval $p_\Lambda = (0.1 - 2.0)$ *GeV/c*, i.e., the results of the Λp enhancement formation experiments. This is demonstrated in *figs. 1,2,3*,and *5*.

2. The peak near the Λp threshold is due to the negative sign Λp scattering length effect at low energy. The negative scattering length excludes the possibility of the existence of (Λp) bound states. The unsuccessful up to now search for the Λ-hyperdeuteron confirms this result.

3. The peaks at 2127 MeV/c^2 and 2257 MeV/c^2 are due to the Λp elastic narrow resonances at 620 and 1120 *MeV/c* of relative Λ-hyperon momenta, respectively (*figs. 2* and *5*).

4. The enhancement near 2184 MeV/c^2 is of kinematical origin and is due to the two-step process $n\,{}^{12}C \to$ $\to (\Sigma N) +$ (Anything), $\Sigma N \to \Lambda p$ (*figs. 3* and *6*).

5. The average range of the Λp interaction forces is about 0.66 *fm*.

6. The components of the average polarization of Λ-hyperons, presumed to be daughters of Λp-systems along the beam direction $- P_z$, normal to the Λp-production

plane $- P_y$ and normal to both these directions $- P_x$, are zero within the limits of errors (lower part of *fig. 1*).

7. It is shown that all these results are very stable with respect to considerable changes of the Λp and ΣN - c.m.s. angular distributions used to model various processes.

The neglect of interference terms in the expressions for the Λp scattering effective cross section, as well as the assumption $\Gamma_{tot} = \Gamma_{el} = \Gamma_R$ and the use of isolated resonance approximation, are justified due to the narrowness of the resonance widths and the total precision of this experiment.

8. It is shown that light nuclei, carbon nucleus at least, could be used as high density nucleon targets to study low energy scattering of unstable particles on nucleons in the absence of monoenergetic beams of such particles.

9. In heavy nuclei one should expect smoothing down, even disappearing of peaks due to the higher probabilities of intranuclear rescattering of hyperons and protons.

10. The effective cross sections of the observed Λp resonances have been estimated: $\sigma^{el}_{\Lambda p}(620) = 12.8$ *mb*, $\sigma^{el}_{\Lambda p}(1120) = 5.61$ *mb*.

11. According to our analysis, a part of protons from the events contributing to the experimental Λp effective mass spectrum, in hyperon-nucleon interactions should arise.

The kinematics of these protons, though produced independently of 1311 lambdas (see 2.1), is different from that of protons of genuine nuclear cascade processes. This means that the form of the background (1) differs from the genuine background formed of lambdas and protons, created in nuclear cascade processes and having never interacted with each other, due to this cause as well.

But this difference cannot, of course, compensate the large difference between the slowly varying background (1) and the peaks arisen in YN-interactions, especially in Λp elastic scattering.

Thus at given total precision of the experiment the form of the background (1) in some extent is not critical.

This has made it possible to obtain self-consistent results.

The authors express their deep gratitude to Prof. A.M.Baldin for his continuous interest and the support of this work.

REFERENCES

1. *B.A.Shahbazian et al. Physics of Elementary Particles and Atomic Nuclei , v. 4, part 3, 811 (1973); Nucl.Phys., B53, 19 (1973); Lett. Nuovo Cimento, v. 6, 63 (1973); JINR, Dubna, E1-7669, 1974.*
2. *Tai Ho Tan. Phys.Rev.Lett., v. 23, 395 (1969); D.T.Cline et al. Phys.Rev.Lett., v. 20, 1452 (1968); D.Eastwood et al. Phys.Rev. D, v. 3, 2603 (1971).*
3. *J.T.Read et al. Phys.Rev., v. 165, 1495 (1968).*
4. *J.A.Kadyk et al. Nucl.Phys., B27, 13 (1971); G.Alexander et al. Phys.Rev., v. 173, 1452 (1968); B.Sechi-Zorn et al. Phys.Rev., v. 175, 1735 (1968); O.Benary et al. A Compilation of YN Reactions, UCRL-20000 YN (1970).*
5. *U.Amaldi et al. Phys.Lett. 25B, 24 (1967).*
6. *J.D.Jackson. Nuovo Cimento, v. 34, No. 6, 1644 (1964).*
7. *G.Alexander. Int. Conf. on Hypernuclear Phys. Argonne, May 5-7, 1969, vol. 1, p. 5.*
8. *J.T.Donohue. Phys.Rev., v. 178, 2289 (1969).*
9. *G.Breit. Theory of Resonance Reactions and Allied Topics, Springer-Verlag, Berlin-Gottingen-Heidelberg, 1959.*

Received by Publishing Department
on August 11, 1976.